Physica 128C (1985) 253–258
North-Holland, Amsterdam

INCOHERENT SCATTERING FUNCTIONS AT INTERMEDIATE ENERGIES AND THEIR DEPENDENCE ON MOMENTUM TRANSFERS

S.V.S. RAMANA REDDY
Department of Physics, Regional Engineering College, Warangal – 506 004 (A.P), India

A. RAGHAVA RAO, K. PREMCHAND, K.L. NARSIMHAM, K. PARTHASARADHI and V. LAKSHMINARAYANA
Laboratories for Nuclear Research, Andhra University, Waltair, India

Received 10 April 1984
Revised 31 July 1984

Incoherent scattering is an important process of interaction of gamma rays with matter at intermediate energies. While enough work has been carried out at large and low momentum transfers (of the gamma ray to the target electron), work on intermediate momentum transfers is limited. With this motivation, a slow-fast coincidence system is developed for studying the incoherent scattering function at intermediate momentum transfers.

1. Introduction

An examination of the entire work carried out in the area of bound electron scattering shows that there is need for a systematic work. Immediately it appeared that while extensive investigations have been carried out at very low and very large momentum transfers, work in the range of intermediate momentum transfers is rather limited. It is therefore decided to choose a range of momentum transfers between 1 to 10 times those of the corresponding electron momenta in the shells and conduct some experiments to obtain information on the effect of binding in incoherent scattering. A given value of the momentum transfer can be realised in a variety of ways in as much as the momentum transfer depends on the scattering angle and incident energy. On an examination of the range of elements used as scatterers it is noticed that most investigations [1–5] were confined to elements of atomic number greater than 50. The reason for this choice was mainly motivated by larger K-X-ray energy which in turn ensures the coincidence efficiency to be close to unity. In the present experiments it is therefore proposed to use scatterers with Z less than 50 and employ an improved coincidence efficiency, close to unity, down to 5 keV. With this motivation the primary photon sources ^{137}Cs (2 Ci) and ^{51}Cr (500 mCi) and scatterers Ag and Zr were selected with an optimised coincidence set-up employing RCA 8575 photomultiplier tubes with NaI(Tl) detectors arranged in a coincidence configuration with an ND512 channel analyser system.

2. Experimental details

In the present studies the coincidence method is employed for studying incoherent scattering functions and the momentum transfer effects to K-shell electrons. Two NaI(Tl) crystals of dimensions 44.45 mm dia. by 50.8 mm height and 44.45 mm dia. by 2 mm height are connected to two photomultipliers (PMT) (RCA 8575). The first detector is used for detecting scattered gamma rays and the second for detection of the K-X-rays. Two lead shields are provided for the detectors to minimise stray coincidences.

The source holder together with the scatterer–detector assembly is shown in fig. 1. A mild steel

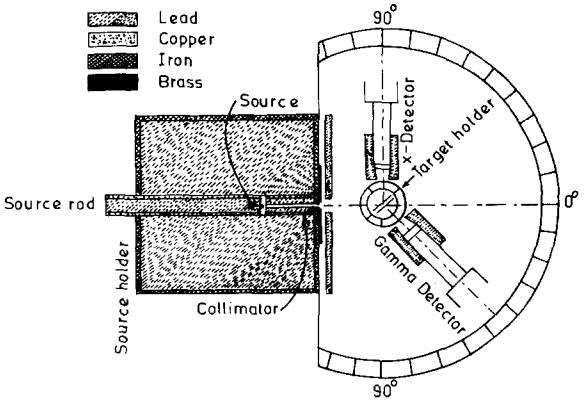

Fig. 1. Source holder and scatterer–detector assembly.

cylinder, 304 mm in length by 304 mm diameter, is filled with lead to house the sources along the axis. Provision is made at one end to have different lead collimators to define various solid angles. The target assembly consists of a target holder in which the experimental foil is held by means of very thin strips of cello-tape and the foil could be easily replaced by lifting the ring with forceps.

Fig. 2 shows the block diagram of the coincidence system. The output from the anodes of the PMT in both cases is used to generate the time logic pulses by constant fraction technique. The fast channel is formed with two constant fraction discriminators (ORTEC Model 473A) and a time-to-pulse-height converter (TPHC) (ORTEC model 467). The output from the

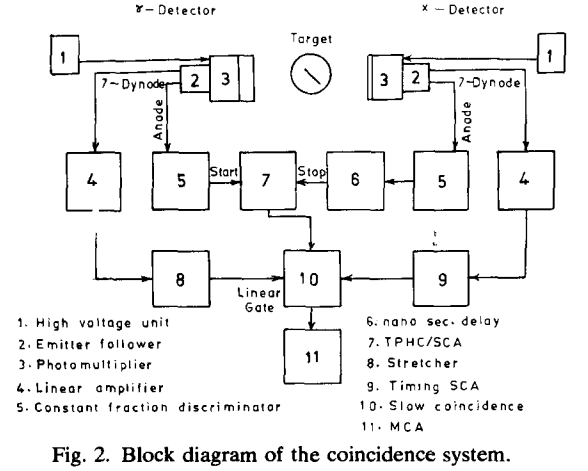

Fig. 2. Block diagram of the coincidence system.

TPHC forms one of the inputs to the slow coincidence unit. The other input to the slow coincidence is derived by gating the bipolar dynode output of the X-ray detector. A timing single channel analyser (SCA) (SC617) is used to select the photo peak of the X-ray in the window. The dynode output from the gamma-ray detector is then fed to the linear gate of the slow coincidence unit through a pulse stretcher (PS 665). The gated output from the gamma detector is stored in the ND512 channel analyser.

Two primary photon sources Cs-137 (2 Ci) and Cr-51 (500 mCi) producing 662 keV and 320 keV, respectively, are used. A silver foil of weight of 105.36 mg/cm^2 and a zirconium foil of weight 64.26 mg/cm^2 are used as scatterers. Foils of different thicknesses of these elements are employed and the experimental foil is selected by optimising the X-ray intensity and the gamma photon intensity. The samples of all the scatterer foils are subjected to chemical analysis and the purity of the samples is found to be better than 99.9 percent.

3. Results and discussion

In this method a pair of NaI(Tl) detectors, connected in a coincidence assembly, is employed. This method yields information exclusively on the effects of binding on K-shell electrons on incoherent scattering. In each Compton process involving a K-shell electron, the electron is either excited or ionised and the incident photon is deflected with decreased energy. In principle, considering the three-body nature of the process, the scattered photon may have an energy anywhere between zero and $h\nu - B_K$, B_K being the binding energy of an electron in the K-shell. The vacancy in the K-shell so created may be filled by one of the outer electrons thereby resulting in the emission of K-X-rays of the scatterer. As mentioned earlier, the X-rays are detected by a thin NaI(Tl) detector and the degraded photons are detected by the thick detector. The coincidence spectrum represents the events caused by incoherent scattering of photons by K-shell electrons only. For a

comparative study the singles spectrum of the scattered photon detector is also recorded separately. These coincidence and the singles spectra, however, include a variety of interfering events, in addition to the desired events. For an accurate evaluation of the final results, these interfering events have to be correctly assessed and subtracted from the respective spectra.

The coincidence spectrum recorded on the multichannel analyser includes chance coincidence events, arising out of the finite resolving time of the coincidence circuit. They can be evaluated from a knowledge of the resolving time of the coincidence circuit and the corresponding singles rates. The coincidence spectrum also includes false coincidence events which may be due to one or more of the following reasons:

(a) The K-X-rays may also be in coincidence with the characteristic Bremsstrahlung arising out of slowing down of the photoelectrons in the scatterer. Similar situations may also be encountered from Compton electrons. The coincidence count rate due to these processes is proportional to the square of the thickness of the target, for thicknesses smaller than the range of Compton or photoelectrons.

(b) The gamma rays scattered from the target and detected in the thick detector may again be scattered and detected in the X-ray detector, depositing an energy corresponding to the range accepted in the window. These crystal-to-crystal scattering events, however, are not considerable in the present studies because of the distances employed and geometries adopted.

(c) Background, scattering in the surrounding objects and higher order effects may cause the recording of events in time coincidence in the two detectors. These events also are relatively scarce.

In any case auxiliary experiments have to be conducted to assess the false events. In the present experimental study these are obtained by placing an equivalent aluminium scatterer in the target position. The coincidence spectrum recorded under identical conditions of the experiment with Ag or Zr foil, can be subtracted from the gross coincidence spectrum observed with Ag or Zr foils to yield the correct coincidence spectrum. Thus the corrected coincidence rate, N_c, is related to the incoherent scattering cross-section of the K-shell electrons by the formula

$$\frac{d\sigma_K}{d\Omega}(\theta) = \frac{N_c}{N_0 \epsilon_y(k) \omega_y \epsilon_x \omega_x \epsilon_c d \gamma_K \nu_{abs}(y_k) \nu_{abs}(x)},$$

where N_c is the true coincidence counting rate due to incoherent scattering K-shell electrons, N_0 the source intensity, ω_y the solid angle subtended by the scattered photon detector at the target, $\epsilon_y(k)$ the efficiency of the scattered photon detector averaged over the spectral range recorded in the detector, ω_x the solid angle subtended by the X-ray detector at the target, ϵ_x the efficiency of the X-ray detector for the detection of K-X-rays, ϵ_c the coincidence efficiency, d the thickness of the target, γ_K the K-fluorescent yield of the target, and $\nu_{abs}(x)$ and $\nu_{abs}(y_k)$ are the absorption factors for the X-rays and gamma rays in the target.

In view of the fact that electrons in Al including those in the K-shell are treated as free, the incoherent scattering cross-section is adequately described by the Klein–Nishina [6] formula:

$$\frac{d\sigma_F}{d\Omega}(\theta) = \frac{N_F}{N_0 \epsilon_y \omega_y d_{Al} \nu_{abs}(y)},$$

where N_F is the number recorded in the scattered spectrum, ϵ_y the efficiency of the photon detector, d_{Al} the number of electrons in the Al target,

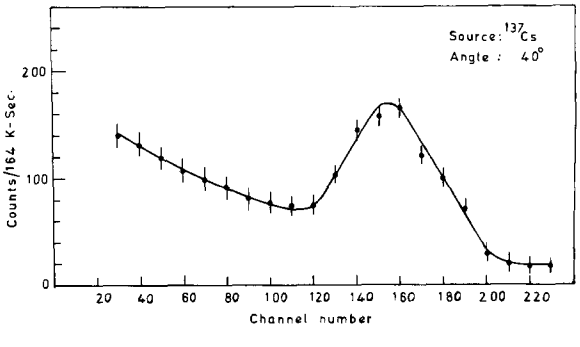

Fig. 3. Typical coincidence system at 40°.

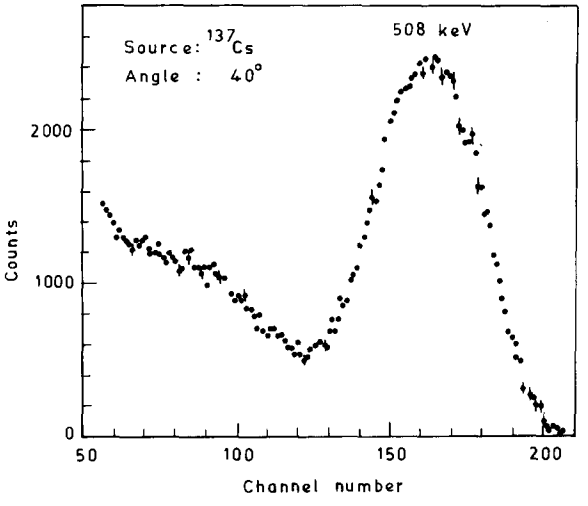

Fig. 4. Typical singles spectrum at 40°.

and $\nu_{abs}(y)$ the absorption fraction in the target.

The incoherent scattering function which is the ratio of the bound-to-free cross-sections is given by

$$\frac{d\sigma_K}{d\sigma_F} = \left[\frac{N_c/\epsilon_y(k)\nu_{abs}(y_k)}{N_F/\epsilon_y\nu_{abs}(y)}\right]\left[\frac{1}{\omega_x\epsilon_x\nu_{abs}(x)}\right] \times \left[\frac{1}{\epsilon_c}\right]\left[\frac{1}{\nu_K}\right]\left[\frac{d_{Al}A}{dA_{Al}}\frac{13}{2}\right],$$

where A and A_{Al} are the atomic numbers of the target element and the aluminium.

A typical coincidence spectrum (with 105.8 mg/cm^2 of Ag foil) and the corresponding singles spectrum (with equivalent Al foil of weight 93.8 mg/cm^2) at 40° are shown in figs. 3 and 4. It may be seen from fig. 3 that even after a counting time of 164 000 s and source intensity of 2 Ci, the individual channels include statistical errors of the order of 10 percent. Part of this error is propagated through the subtractions of the chance and false coincidences. This procedure is repeated for all the other angles using the two different target elements and the two sources. The values of the incoherent scattering function $d\sigma_K/d\sigma_F$ in each case for the two sources are given in tables I and II.

The results of the coincidence experiments at 662 keV in the angular range 40° to 100° for Ag and Zr scatterers are compared with the theoretically estimated corresponding ratios using Hubbell's tables [7] and the relativistic equations of Jauch and Rohrlich [8]. The experimental incoherent scattering function in the case of Ag is found to vary from 0.7 to 1.32 in the angular range investigated, the corresponding variation for Zr scatterers in the same range being 0.80 to 1.48. Considering the experimental errors, the variations in the two elements are of the same order. In the case of incident photons of 320 keV the ratios of Ag and Zr varied from 0.61 to 1.14 and from 0.97 to 1.53, respectively. Here also, considering the experimental errors, the range of variation is the same. Thus the general trend of variation of the incoherent scattering function is that it goes to low values for low momentum transfers, in general agreement with the trends observed in the earlier experiments for heavy elements. It is interesting to note that the values of forward angles of scattering differ considerably (as much as 40 percent) from the non-relativistic Hartree–Fock estimates, included in Hubbell's tables. It is also interesting to note that the values of the incoherent scattering function are considerably larger at backward angles than those predicted by the relativistic estimates of Jauch and Rohrlich. The deviation for low momentum transfers may be attributed to the fact that the present values are exclusively for K-shell electrons, while the values tabulated by Hubbell are for all the electrons in an atom.

It is instructive to study the dependence of the present experimental values of the incoherent scattering function on the momentum transfer to the electron. For this purpose the values of momentum transfer at all angles of scattering are estimated, both at 662 keV and at 320 keV. Ratios 'r' are formed for this momentum transfer with the momentum of the electron in the K-shell. A double ratio 'R' is formed with this ratio and the incoherent scattering function. Plots for the four cases studied are shown in fig. 5. It can be seen from these plots that both the ratios have the same trend of variation with angle. However, the corresponding slopes of variation are different. A smaller slope for the double ratio is indicative of larger

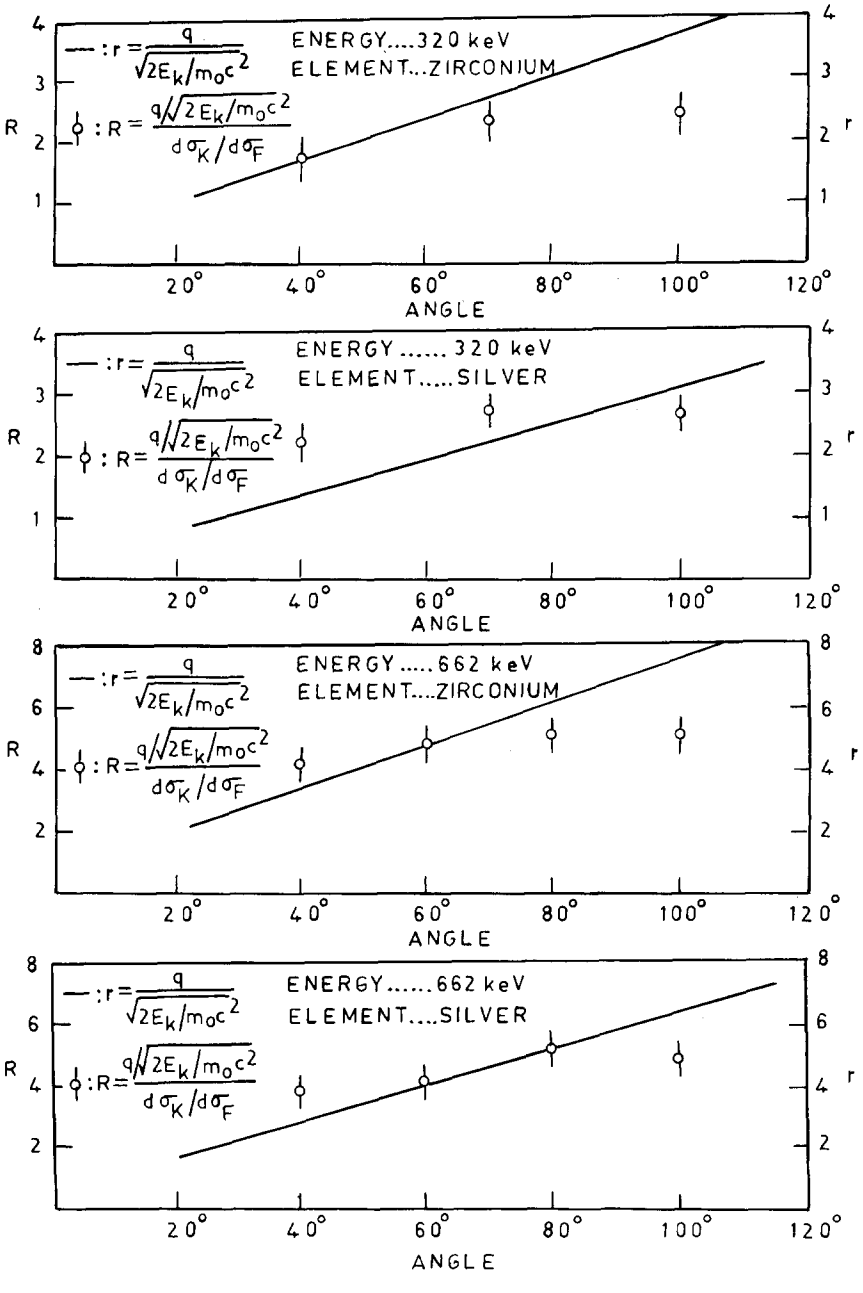

Fig. 5. Ratios of momentum transfers at various angles of scattering.

Table I
Incoherent scattering functions at 662 keV

		Silver			Zirconium		
			Theoretical values			Theoretical values	
Sl. No.	Scattering angle	Experimental value	Jauch and Rohrlich	Hubbel	Experimental value	Jauch and Rohrlich	Hubbel
1	40°	0.724(34)	0.968	0.998	0.796(29)	0.975	0.999
2	60°	0.994(35)	0.982	0.999	1.012(31)	0.999	0.999
3	80°	1.048(45)	1.040	0.999	1.243(50)	1.026	0.999
4	100°	1.323(83)	1.100	0.999	1.477(112)	1.076	0.999

Table II
Incoherent scattering functions at 320 keV

		Silver			Zirconium		
			Theoretical values			Theoretical values	
Sl. No.	Scattering angle	Experimental value	Jauch and Rohrlich	Hubbel	Experimental value	Jauch and Rohrlich	Hubbel
1	40°	0.609(97)	0.970	0.982	0.966(174)	0.977	0.987
2	70°	0.845(101)	1.007	0.997	1.185(198)	1.004	0.998
3	100°	1.141(154)	1.168	0.999	1.534(276)	1.040	0.999

values of the incoherent scattering function at larger angles of scattering, which is an unexpected result.

References

[1] Z. Sujkowski and B. Nagel, Ark. Phys. 20 (1961) 323.
[2] J.W. Motz and G. Missoni, Phys. Rev. 124 (1961) 1458.
[3] J. Verma and M.A. Eswaran, Phys. Rev. 127 (1962) 1197.
[4] S. Shimizu, Y. Nakayama and T. Mukoyama, Phys. Rev. A140 (1965) 806.
[5] O. Pingot, Nucl. Phys. A119 (1968) 667.
[6] O. Klein and Y. Nishina, Z. Physik 52 (1929) 853.
[7] J.H. Hubbell, Wm.J. Veigele, E.A. Briggs, R.T. Brown, D.T. Cromer and R.J. Howerton, J. Phys. Chem. Ref. Data, Vol. 4, No. 3 (1975).
[8] J.M. Jauch and F. Rohrlich, The Theory of Photons and Electrons (Addison-Wesley, Cambridge, Mass., 1955).